Published in final edited form as:
Stem Cells. 2013 August ; 31(8): 1669–1682. doi:10.1002/stem.1416.

Abi3bp is a multifunctional autocrine/paracrine factor that regulates mesenchymal stem cell biology

Conrad P Hodgkinson[1], **Vinogran Naidoo**[1], **Karl G Patti**[1], **Jose A Gomez**[1], **Jeffrey Schmeckpeper**[1], **Zhiping Zhang**[1], **Bryce Davis**[1], **Richard E Pratt**[1], **Maria Mirotsou**[1], and **Victor J Dzau**[1]

[1]Mandel Center for Hypertension Research and Division of Cardiovascular Medicine, Department of Medicine, Duke University Medical Center, Durham, NC 27710, USA

Abstract

Mesenchymal stem cells (MSCs) transplanted into injured myocardium promote repair through paracrine mechanisms. We have previously shown that MSCs overexpressing AKT1 (Akt-MSCs) exhibit enhanced properties for cardiac repair. In this study, we investigated the relevance of Abi3bp towards MSC biology. Abi3bp formed extracellular deposits with expression controlled by Akt1 and ubiquitin-mediated degradation. Abi3bp knockdown/knockout stabilized focal adhesions and promoted stress-fiber formation. Furthermore, MSCs from Abi3bp knockout mice displayed severe deficiencies in osteogenic and adipogenic differentiation. Knockout or stable knockdown of Abi3bp increased MSC and Akt-MSC proliferation, promoting S-phase entry via cyclin-d1, ERK1/2 and Src. Upon Abi3bp binding to integrin-β1 Src associated with paxillin which inhibited proliferation. In vivo, Abi3bp knockout increased MSC number and proliferation in bone marrow, lung, and liver. In summary, we have identified a novel extracellular matrix protein necessary for the switch from proliferation to differentiation in MSCs.

Keywords

mesenchymal stem cells; extracellular matrix; integrin; cell signaling

Introduction

Stem cell therapy for tissue repair and regeneration has great therapeutic potential [1-4]. Adult stem cells from the bone marrow are one of the most widely used cells for this purpose. Bone marrow contains a heterogeneous population of cells, including mesenchymal stem cells (MSCs), or marrow stromal stem cells. MSCs are non-hematopoietic stem cells that have the potential to develop into differentiated cell types such as osteocytes, chondrocytes, and adipocytes as well as nerve cells [5]. One of the major issues regarding the therapeutic potential of MSCs is their poor survivability *in vivo*. To this end our

Corresponding author: Victor J Dzau M.D., Mandel Center for Hypertension Research and Division of Cardiovascular Medicine, Department of Medicine, Duke University Medical Center, Durham, NC 27710, USA. victor.dzau@duke.edu.

Contributions: Conrad P Hodgkinson: conception and design, collection of data, data analysis and interpretation, manuscript writing, final approval of manuscript. Vinogran Naidoo: collection and/or assembly of data. Karl G Patti: collection and/or assembly of data. Jose Gomez: collection and/or assembly of data. Jeffrey Schmeckpeper: collection and/or assembly of data. Zhiping Zhang: collection and/or assembly of data. Bryce Davis: collection and/or assembly of data. Richard Pratt: data analysis and interpretation. Maria Mirotsou: conception and design, manuscript writing, final approval of manuscript. Victor J Dzau: conception and design, manuscript writing, data analysis and interpretation, final approval of manuscript.

Conflict of Interest
No author listed above has a conflict of interest with this study.

laboratory over-expressed the Akt1 oncogene in MSCs. Injection of Akt1 modified MSCs into the heart after myocardial infarction increased MSC survival and led to major reduction in infarct size, associated with significant improvements in cardiac function [6]. Further research revealed that these therapeutic effects were mediated in part by the release of paracrine factors by these cells. Validation of this paracrine mechanism came from *in vivo* experiments where concentrated media from Akt1 modified MSCs reduced infarct size and cardiac cell apoptosis in a rat coronary occlusion model [6]. A functional genomic strategy identified several novel proteins that were regulated by Akt1 and potentially could account for the enhanced therapeutic properties of the Akt-MSCs. One of these novel proteins was Abi3bp [7].

Abi3bp is a relatively novel protein for which the biological function is unclear. A partial fragment of Abi3bp, also known as TARSH and eratin, was identified in a yeast two-hybrid screen with the c-Abl binding protein Abi3 as bait [8]. However, *in vivo* binding activity between full-length Abi3bp and Abi3 awaits confirmation. Expression of the protein has been observed in the olfactory system; conditioned media containing Abi3bp reduced mitral cell dendritic complexity, which is an important step in the formation of functional circuits [9]. Computational screening followed by *in vitro* assays identified that a partial fragment of Abi3bp, containing one of the two Fibronectin type-III domains found in the full length protein, promoted cell attachment and was capable of assembling into an extracellular matrix [10]. In addition, Abi3bp is expressed in normal thyroid and in benign follicular thyroid adenoma but is absent in follicular thyroid carcinoma [11]. Similarly, loss of Abi3bp RNA expression has been reported in both lung cancer cell-lines and lung tumor specimens [12]. Abi3bp has been reported to have both a positive and negative role in senescence [13, 14]. In this study we show that Abi3bp plays an important role in MSC biology by acting as a “check and balance” in many MSC processes including proliferation, differentiation, adhesion, morphology and transformation.

Materials and Methods

Full Methods are given in the Supplementary

Abi3bp knockout mice

Abi3bp$^{-/+}$ mice, harboring a neoR replacement of the first exon, were purchased from Taconic. All experiments were performed with littermates and in accordance with institutional guidelines (DLAR and IACUC).

Mesenchymal stem cell isolation and retroviral transfection

Bone marrow cells from eight 8-week-old wild-type male C57BL/6J mice (Jackson Laboratory) or from three 8-week old male Abi3bp wild-type and knockout mice were collected in MEMα (Invitrogen) supplemented with 20%v/v heat-inactivated FBS and 1x penicillin-streptomycin (Invitrogen) by flushing the marrow cavity with a 27-guage needle. Cells were filtered through a 40μm cell strainer (Falcon). Mononuclear cells then were isolated from aspirates by Ficoll-Paque (GE Healthcare) gradient centrifugation and cultured. Cells were plated at a density of $20\times10^6/9.5cm^2$. Mesenchymal stem cells (MSCs) were separated from hematopoietic cells based on their preferential attachment to cell culture surfaces. Non-adherent cells were removed 24 hours after plating and the adherent layer washed twice in culture media (MEMα supplemented with 20% v/v heat-inactivated FBS and 1x penicillin-streptomycin). Media was changed every two days and once MSCs were 70% confluent cells were removed by 0.05% v/v trypsin and re-plated at 5000 cells/cm^2. MSCs were cultured in this fashion until used in an experiment. MSC isolations were performed from Abi3bp wild-type and knockout mice on three separate occasions. In the

first isolation MSCs were used at passage 10, MSCs from the subsequent two isolations were used at passage 5. MSCs at this passage were tested for various MSC, haematopoietic, and endothelial markers as described in the results section. MSC senescence was evaluated by β-galactosidase staining (Cell Signaling). Lung and liver MSCs were isolated by FACS sorting and cultured according to the bone marrow protocol. Differentiation potential of the lung and liver MSCs were evaluated at passage 5.

MSC differentiation

For smooth muscle differentiation MSCs were seeded at 5000 cells/cm^2 in normal growth medium. The next day media was changed for DMEM+10% heat-inactivated FBS supplemented with 10ng/ml TGF-β and 50ng/ml PDGF. Media was changed every two days for a total of six days, whereupon the cells were fixed and analyzed for smooth muscle actin by immunofluorescence (α-smooth muscle actin, Sigma). For osteogenic differentiation MSCs were seeded at 10000 cells/cm^2 in normal growth medium. The next day media was changed for DMEM+10% heat-inactivated FBS supplemented with 1μM dexamethasone and 25μg/ml ascorbic acid-2-phosphate. Media was changed every two days for a total of four weeks, cells were fixed, and analysed for osteogenesis using 2% Alizarin-Red (pH4.2). For chrondrogenic differentiation MSCs were resuspended at a concentration of 1.6×10^7 cells/ml. 5μl aliquots were seeded into 12-well plates and left in a humidified atmosphere for two hours. Differentiation media with or without chrondrogenic supplement (R&D Systems) was added. Media was changed every four days for a total of two weeks, cells were fixed, and analysed for chrondrogenesis using 1% Alcian-Blue in 0.1M HCl.

siRNA transfection

siRNA pools and the negative control were purchased from Dharmacon. Transfection was carried out with Dharmafect-I (Dharmacon) according to manufacturer's guidelines. Full details are supplied in the Supplemental Methods.

qPCR

Total RNA was extracted using a Rneasy Plus Micro Kit according to the manufacturer's guidelines (Qiagen). Total RNA (500ng) was converted to cDNA using a high capacity cDNA reverse transcription kit (Applied Biosystems). qPCR was performed by incubating cDNA with a FAM conjugated gene specific primer and TaqMan Gene Expression Master Mix (Applied Biosystems).

Immunofluorescence

The staining procedure is described in the Supplemental Methods.

Cell counting

Cell counting was performed with Promega CellTiter 96 Aqueous Non-Radioactive Cell Proliferation Assay (MTS) according to the manufacturer's guidelines. Incubations were all 90 minutes at 37°C. MSC cell lines were all seeded at 5000 cells per cm^2 and a 48-well format was used.

Fluorescence-activated cell sorting

The antibodies and methods employed are described in the Supplemental Methods.

Co-immunoprecipitation

Co-immunoprecipitation was performed as described previously [15].

Images

Figures were prepared using CorelDraw. Microscopy images were exported from Axiovision Rel4.8 software. For brightfield images, where necessary colour casts were removed using Photoshop using a pure white area of the photo.

Statistics

Statistical analysis was performed with GraphPad or R. Experiments containing two conditions a t-test was performed. ANOVA was used for experiments with three or more conditions followed by Bonferroni post-hoc tests for comparisons between individual groups.

Results

Abi3bp is an extracellular matrix protein controlled by Akt and ubiquitin

Previous work in our laboratory identified that MSCs modified to over-express the oncogene Akt1 show enhanced survival and release of cytoprotective and angiogenic factors after transplantation into the injured myocardium [6]. Microarray analysis found a number of genes of relatively unknown function that were positively induced by Akt1 [7]. One of these genes was Abi3bp.

In-order to validate the microarray data we first performed qPCR using MSC, MSC-GFP, and MSC-GFP-Akt1 cells cultured *in vitro*. Akt1 over-expression in MSCs increased Abi3bp RNA levels by ~20-fold when compared to MSC and MSC-GFP cells (Figure 1A). This was accompanied by an increase in Abi3bp protein levels, albeit less dramatic (Figure 1A). To further test whether Akt1 regulated Abi3bp expression we used a pool of 4 siRNAs targeted against Akt1 to deplete the protein from MSC-GFP-Akt1 cells. When Akt1 was depleted Abi3bp RNA expression was reduced by ~10-fold, validating that Akt1 regulates Abi3bp expression (Figure 1B). Finally, insulin stimulation following a period of serum withdrawal activated endogenous Akt in MSCs and increased Abi3bp expression when compared to control untreated cells (Figure 1C).

Akt1 had a substantially greater effect on Abi3bp RNA expression than on the protein, suggesting that a post-translational mechanism regulates Abi3bp levels. To test this hypothesis we generated a HEK293 cell-line which over-expressed a myc-tagged Abi3bp construct. These cells were treated with either vehicle or the proteasome inhibitor clasto-lactacystin β-lactone for 24 hours after which the cells were exposed to cycloheximide, an inhibitor of protein synthesis. In the presence of cycloheximide alone the half-life of the myc-tagged Abi3bp was ~1hr (Figure 1D). Clasto-lactacystin β-lactone had a dramatic effect, increasing expression of Abi3bp by ~5-fold. When cells were cultured in both cycloheximide and clasto-lactacystin β-lactone, levels of the myc-tagged Abi3bp did not significantly decrease during the length of the experiment, indicating a half-life in excess of 8 hours (Figure 1D). Taken together this data indicates that Abi3bp undergoes rapid degradation by a ubiquitin mediated process.

A previous study has shown that a partial fragment of Abi3bp formed pericellular deposits typical of extracellular matrix (ECM) deposition [10]. We were interested to determine whether the full-length protein would behave in a similar fashion. Abi3bp was secreted by HEK293 cells over-expressing the protein (Figure 1E). Surfaces exposed to HEK293 cells expressing myc-tagged Abi3bp showed strong ECM staining with a myc-antibody. This was not observed on surfaces exposed to HEK293 cells expressing the control vector (Figure 1E).

Abi3bp controls MSC cell biology, differentiation, and motility

Focal complexes (FC) are small dot-like adhesions that are the first points of contact between the cell and the extracellular matrix. FC are transient, and if not stabilized into focal adhesions (FA), are quickly broken down [16-18]. Focal adhesion turnover is very important for cell spreading, migration and proliferation. We investigated whether Abi3bp affects focal adhesion formation using three cell systems: (i) MSC or (ii) MSC-GFP-Akt1 cells expressing either the scrambled control shRNA or the Abi3bp shRNA-83 or (iii) MSCs from wild-type and Abi3bp knockout mice. Abi3bp knockdown was achieved by stably expressing one of two shRNA constructs, sh91 or sh83. Stable expression of a scrambled shRNA was used as a control (Supplementary Figure 1A). The wild-type and Abi3bp knockout MSCs used in this study were primary cells as they displayed senescence (Supplementary Figure 1B). Analysis of cell surface markers showed that the MSC isolations were free of hematopoietic and endothelial contamination (no expression of CD45, CD11b, CD34, and CD31- Supplementary Figure 2). Cells were stained with several FC/FA markers, these being phospho-Y118 paxillin and paxillin. Cells were also incubated with phalloidin to stain F-actin stress fibers. Abi3bp knockout MSCs were found to have a significantly lower phospho-paxillin/paxillin ratio for stained foci area, whereas phalloidin intensity was increased when compared to control MSCs (Figure 1F top). Similar findings were observed in the MSC-GFP-Akt1 system (Figure 1F, bottom) and in this cell model phospho-paxillin to vinculin ratios were nearly identical to those for phospho-paxillin:paxillin (Supplementary Figure 1C). Other parameters are shown in Supplementary Figure 1D.

MSCs have the potential to differentiate into several cell types. We investigated whether Abi3bp was important in this process. All three MSCs isolations from wild-type or Abi3bp knockout mice were induced with dexamethasone and ascorbic acid for osteogenesis. All of the wild-type MSC isolations were capable of undergoing osteogenic differentiation as evidenced by robust alizarin-red staining. Normalization to cell number showed a >20-fold increase in alizarin red staining in the treated wild-type MSCs (Figure 2A). However, all three Abi3bp knockout MSC isolations completely failed to show any significant alizarin-red deposition both visually and after normalization to cell number (Figure 2A). We subsequently measured Runx2 expression, an early marker of commitment to the osteogenic lineage, in our wild-type and Abi3bp knockout MSCs. Wild-type MSCs cultured in differentiation media had a significant 2-fold increase in Runx2 expression when compared to the vehicle control (Figure 2A, right hand panel). However, though Runx2 expression in the treated Abi3bp knockout MSCs was higher when compared to vehicle control cells the increase was not significant (Figure 2A, right hand panel). Furthermore, Runx2 expression in the Abi3bp knockout MSCs was significantly lower than wild-type cells. This data suggests that Abi3bp knockout affects early commitment to osteogenic differentiation. The wild-type MSC isolations also showed robust chrondrogenic differentiation; the cells formed pellets with strong deposition of proteoglycans as shown by Alcian Blue staining and normalization to cell number (Figure 2B, Supplementary Figure 1E). In contrast Abi3bp knockout MSCs did not form chrondrogenic pellets instead forming a cellular net. Normalization to cell number indicated that in contrast to wild-type MSCs proteoglycan deposition in Abi3bp knockout MSCs was highly variable (Figure 2B). Both wild-type and Abi3bp knockout MSCs were capable of differentiating into smooth muscle, however the general appearance of the cells was substantively different between the two cell types (Figure 2C). Finally, we measured adipogenic differentiation in our MSC isolations. All three wild-type MSC isolations generated adipocytes (Figure 2D). The first isolation had the smallest fold increase, which may be due to their higher passage number. In contrast Abi3bp knockout MSCs were severely limited in their ability to differentiate into adipocytes (Figure 2D). Considering that Abi3bp controls focal adhesion formation we investigated whether

this protein also affected MSC movement. Using a scratch assay MSCs lacking Abi3bp showed higher motility when compared to control cells (Figure 2E, Supplementary Figure 1F). One might expect MSCs lacking Abi3bp to have a slower motility because of the stabilization of the focal adhesions in these cells. However these cells were found to have a higher proliferation rate (see below) and this result may be due to an increase in cell number rather than representing more motile cells.

Abi3bp controls MSC proliferation

Considering that cell shape is an important determinant for proliferation we hypothesized that Abi3bp would control this process in MSCs.

Prior to testing this hypothesis we first characterized MSC, MSC-GFP, and MSC-GFP-Akt1 growth curves using a MTS assay to measure cell number. Both MSC and MSC-GFP cells had virtually identical growth curves (Supplementary Figure 3A, Supplementary Table I). Over-expression of the Akt1 oncogene increased MSC growth rate ~4 fold (Supplementary Table I).

Comparing the growth rates of the wild-type and Abi3bp knockout MSCs indicated that all three Abi3bp knockout MSCs isolations possessed a higher growth rate when compared to their wild-type MSC counterparts (Figure 3A). Averaging the growth rates of the respective isolations showed that wild-type MSCs have a significantly slower growth rate than Abi3bp knockout MSCs (Figure 3A). Additional experiments with shRNA showed that Abi3bp knockdown increased the growth rate of MSCs by ~2-fold (Supplementary Table I, Figure 3B) and by ~3-fold for MSC-GFP-Akt1 cells (Supplementary Table I, Figure 3B, Supplementary Figure 3B).

Various assays were employed to determine if the effects on cell number were due to changes in cell cycle and proliferation. Flow cytometry was used to measure the percentage of wild-type and Abi3bp knockout MSCs undergoing active proliferation in culture. All three Abi3bp knockout MSC isolations displayed ~2-fold higher incorporation of BrdU, a thymidine analogue, when compared to the wild-type MSC controls (Figure 3C) indicating that Abi3bp knockout increased proliferation. Validation experiments were performed with shRNA knockdown. In MSCs incubated with BrdU Abi3bp knockdown increased the percentage of cells in S-phase (Figure 3D, Supplementary Figure 3C). Similarly, knockdown of Abi3bp by either shRNA construct in MSC-GFP-Akt1 cells caused a significant increase in the incorporation of BrdU as determined by ELISA (Supplementary Figure 3D). Flow cytometry was used to further investigate the cell cycle. MSC-GFP-Akt1 DNA was stained with 7-AAD and cells ascribed to a phase of the cell cycle using a Watson model. In control MSC-GFP-Akt1 cells the number of cells in S-phase was ~2.5-fold lower when compared to cells lacking Abi3bp (Figure 3E). The number of cells in G0/G1 was significantly lower in the Abi3bp knockdown cells, however no effect was observed on the G2/M population (Figure 3E). Effects on the cell cycle were also evaluated by flow cytometry using cells incubated with BrdU. Again Abi3bp knockdown in MSC-GFP-Akt1 cells increased the number of cells in S-phase with a concomitant decrease in G0/G1-phase. No effect was observed on G2/M (Figure 3F). Finally, immunostaining MSC-GFP-Akt1 cells indicated a greater percentage of cells expressing the marker Ki67, which is expressed only during the active phase of the cell cycle, in Abi3bp knockdown cells when compared to the scrambled control (Figure 3G). Concentrated media prepared from HEK293 cells expressing the myc-tagged Abi3bp inhibited proliferation of both MSC and MSC-GFP-Akt1 cells when compared to control concentrated media (Supplementary Figure 3E) further validating the anti-proliferative effect of Abi3bp.

Having ascertained that Abi3bp controlled MSC proliferation we then wished to determine the mechanism.

Entry into the cell cycle is controlled by the expression of various cyclins. One of the most important is cyclin-d1. As shown in Figure 4A all three Abi3bp knockout MSC isolations possessed significantly higher cyclin-d1 expression when compared to their wild-type counterparts (Figure 4A, Supplementary Figure 4A). The same result was observed in the knockdown system. As shown in Figure 4B, in control MSC-GFP-Akt1 cells, which expressed the scrambled shRNA, cyclin-d1 expression progressively decreased during culture; by day 2 cyclin-d1 levels were ~30% of basal. Knockdown of Abi3bp prevented any loss of cyclin-d1 expression. To verify that cyclin-d1 expression affects MSC-GFP-Akt1 proliferation stable cell-lines were generated expressing either a control- or a myc-DDK-tagged cyclin-d1 vector (Supplementary Figure 4B). Over-expression of the myc-DDK-tagged cyclin-d1 significantly increased cell number in culture and the number of cells in S-phase (Supplementary Figure 4B).

Cyclin-d1 expression is commonly controlled by MAPKs such as ERK. Abi3bp knockout increased p-ERK at both one and two days post-seeding in all three MSC isolations when compared to wild-type control cells (Figure 4A, Supplementary Figure 4A). Similarly, Abi3bp knockdown in MSC-GFP-Akt1 cells increased phospho-ERK2 levels when compared to control cells. Furthermore Abi3bp knockdown prevented the de-phosphorylation observed in the control cells (Figure 4B). A similar effect was observed with ERK1 but the data did not reach statistical significance. To ascertain whether ERK could affect MSC proliferation, cells of the model MSC-GFP-Akt1 system were made to stably express either a scrambled control shRNA or a shRNA that targeted ERK2, the major ERK isoform in MSCs. Of the two shRNAs ERK2-shRNA-76 gave the highest level of ERK2 depletion (Figure 4C, left panel) and had the greatest inhibitory effect on cyclin-d1 expression (Figure 4C), number of cells in S-phase (Figure 4C) and growth rate (Figure 4C, right panels and Supplementary Table I). Similarly, ERK2-shRNA-76 expression in MSC-GFP-Akt1 cells increased the number of cells in G0/G1 (Supplementary Figure 4C). The growth rate of the MSC-GFP-Akt1 cells expressing the ERK2-shRNA-sh76 was virtually identical to unmodified MSCs underlying the importance of ERK for MSC proliferation.

MEK is the upstream activator of ERK; the MEK inhibitors U0126 and PD98059 were used to confirm the ERK knockdown experiment and the role of ERK in MSC proliferation. Both U0126 and PD98059 inhibited ERK phosphorylation and cyclin-d1 expression in MSC-GFP-Akt1 cells as determined by immunoblotting (Supplementary Figure 5A). The MEK inhibitors significantly decreased the number of MSC and MSC-GFP-Akt1 cells in S-phase as determined by BrdU incorporation and flow cytometry (Supplementary Figure 5B) further underlining the importance of the ERK pathway in MSC proliferation.

Paxillin phosphorylation, which earlier we showed was regulated by Abi3bp, has been previously correlated both negatively and positively with ERK phosphorylation depending upon cell type [19, 20]. We first verified the staining experiment by immunoblotting. Paxillin phosphorylation at Y188 was found to be negatively regulated by Abi3bp; at both one and two days post-seeding pY118-paxillin was significantly lower in all three Abi3bp knockout MSC isolations when compared to control cells (Figure 5A, Supplementary Figure 5C). pY118-paxillin increased ~60-fold in control MSC-GFP-Akt1 cells. However in Abi3bp knockdown MSC-GFP-Akt1 cells paxillin-Y118 phosphorylation was substantially reduced; at day 2 post-seeding paxillin-Y118 phosphorylation was only ~10-fold above basal (Figure 5B). We then wished to determine whether there was any link between paxillin and ERK phosphorylation (Figure 5C). Transfection of MSC-GFP-Akt1 cells with a siRNA pool depleted paxillin protein by over 90% (Figure 5D, Supplementary Figure 6A).

Interestingly phospho-ERK1/2 levels were dramatically increased in the paxillin siRNA treated cells. These effects were not due to transfection or the lipid carrier, neither transfection of a negative siRNA control or the lipid alone had any effect on paxillin, phospho-ERK1/2, or actin (Figure 5D). This effect was specific to paxillin, knockdown of another focal adhesion protein, vinculin, had no effect on p-ERK (Figure 5D). Taken together this indicated that paxillin was sequestering a kinase capable of activating the ERK pathway.

The MEK-ERK pathway is activated by Ras and we determined the activity of this protein by incubating agarose beads coupled to the ras binding domain of Raf-1, which preferentially binds to the active GTP bound form of ras, using MSC-GFP-Akt1 protein extracts from control and Abi3bp knockdown cells. Ras activity was found to be significantly increased by Abi3bp knockdown (Figure 5E). Ras itself is controlled by various pathways, including Grb2-SOS and Src. Grb2-SOS was found not to be important for Ras-MEK-ERK activation in MSCs, peptide mediated disruption of the Grb2-SOS association had no effect on ERK phosphorylation (Figure 5E). Inhibition of Src by the inhibitor PP2A inhibited ERK phosphorylation, cyclin-d1 expression, and entry into S-phase (Figure 5F and 5G, Supplementary Figure 6B) in both MSCs and Akt-MSCs indicating that this tyrosine kinase was responsible for activating the Ras-MEK-ERK pathway.

We then wished to determine how Src was the kinase being sequestered by paxillin. The experiments above showed that Abi3bp knockdown decreased phospho-Y188-paxillin. Considering that paxillin-Y118 phosphorylation is mediated by Src this was an avenue we explored further. Co-immunoprecipitation experiments were used to verify this hypothesis. In control MSC-GFP-Akt1 cells Src co-precipitated with paxillin at both one and two-days post seeding (Figure 6A). In contrast to the control cells, in MSC-GFP-Akt1 cells lacking Abi3bp the levels of co-precipitated Src were substantially reduced; indicating increased availability of Src which could potentially activate the ERK pathway (Figure 6A). No co-immunoprecipitation of Src was observed with isotype control antibody (Figure 6A). Src immunoprecipitates contained equal amounts of Raf-1, a Src target [21], in control and Abi3bp knockdown MSC-GFP-Akt1 cells (Figure 6B) indicating that Abi3bp does not control ERK phosphorylation through Src activation of Raf-1.

Abi3bp binds to integrin-β1

Given the extracellular nature of Abi3bp and the observation that the protein affected focal adhesion formation and related signaling pathways, we surmised that Abi3bp could modulate growth-factor and/or integrin receptors. Abi3bp did not affect growth-factor signaling; equivalent p-ERK1/2 levels were observed in serum starved MSC-GFP-Akt1 cells stimulated with conditioned media prepared from HEK293 cells expressing either a control vector or the myc-tagged Abi3bp vector (Figure 6C). If the Abi3bp receptor was an integrin, blocking antibodies would increase ERK phosphorylation. We chose to investigate three integrins, α4, α5, and β1 as they are commonly expressed by MSCs. Compared to untreated cells incubation with the isotype control, α4 and α5 blocking antibodies had no effect on ERK phosphorylation. However, incubation with the β1 blocking antibody increased phospho-ERK1/2 levels ~3.5-fold. Co-incubation of the β1 blocking antibody with either α4 or α5 blocking antibody had comparable effects to the β1 antibody alone (Figure 6D). This result suggested that β1 could be a Abi3bp receptor. To determine if direct binding could be observed between Abi3bp and integrin-β1 pull-down experiments were performed. Protein extracts from MSC-GFP-Akt1 cells were incubated with conditioned media prepared from fresh serum-free media, serum-free media exposed to HEK293 cells expressing a control vector, or serum-free media exposed to HEK293 cells expressing the myc-tagged Abi3bp vector. Immunoprecipitation with myc resulted in the co-precipitation of integrin-β1 only when myc-tagged Abi3bp was present (Figure 6E). This experiment was further verified;

immunoprecipitation of endogenous Abi3bp from MSC-GFP-Akt1 cells resulted in the co-precipitation of integrin-β1 (Figure 6E, right panel).

Mice lacking Abi3bp show aberrant MSC proliferation

Having shown that both Abi3bp knockout and knockdown increased MSC proliferation *in vitro* we hypothesized that Abi3bp knockout would affect MSC proliferation *in vivo*. Abi3bp is expressed in most tissues but is highest in the lung (Supplementary Figure 7A). We analyzed MSC populations by flow cytometry and measured proliferation by BrdU uptake. In the bone marrow we investigated MSCs using two sets of markers; $CD45^{neg}CD44^{pos}CD105^{pos}$ and $CD45^{neg}Sca\text{-}1^{pos}$ as CD44, CD105, and Sca-1 are known to be expressed on mouse MSCs. First we needed to confirm that $CD45^{neg}CD44^{pos}CD105^{pos}$ are indeed MSCs. As shown in Supplemental Figure 8A $CD45^{neg}CD44^{pos}CD105^{pos}$ cells in both wild-type and knockout animals express Sca-1, a mouse MSC marker, but do not possess hematopoietic (CD45, CD34) or endothelial markers (CD31) indicating that the $CD45^{neg}CD44^{pos}CD105^{pos}$ population are MSCs. $CD45^{neg}CD44^{pos}CD105^{pos}$ number was increased by Abi3bp knockout (Figure 7A). Furthermore, Abi3bp knockout enhanced the proliferation of these cells as shown by the ~3-fold increase in BrdU incorporation (Figure 7B). Similarly, the proliferation rate of $CD45^{neg}Sca\text{-}1^{pos}$ cells was increased in the Abi3bp knockout bone marrow (Figure 7C). We wanted to see if the cultured MSCs were related to the *in vivo* MSCs we had characterized. Indeed we found that $CD45^{neg}CD44^{pos}$ cells are enriched in the tissue culture plastic attached population following 12 hours of culture, suggesting that the $CD45^{neg}CD44^{pos}CD105^{pos}$ give rise to the cultured MSCs we investigated above (Supplementary Figure 8B). In the liver we investigated two MSC populations, $CD45^{neg}CD73^{pos}CD90^{pos}CD105^{pos}$ and $CD45^{neg}Sca\text{-}1^{pos}$. Akin to the bone marrow liver $CD45^{neg}CD73^{pos}CD90^{pos}CD105^{pos}$ MSCs were elevated in the Abi3bp knockout animal (Figure 7D). Further analysis using BrdU showed that MSCs were ~3.5fold more proliferative in the absence of Abi3bp (Figure 7E). Similarly, Abi3bp knockdown increased the proliferation of liver $CD45^{neg}Sca\text{-}1^{pos}$ MSCs (Figure 7F). Analogous to the liver, lung $CD45^{neg}$ $CD73^{pos}$ $CD90^{pos}$ $CD105^{pos}$ MSC numbers were elevated and more proliferative in the Abi3bp knockout animal (Figure 7G, Supplemental Figure 9B). No effect was observed with the kidney $CD45^{neg}CD73^{pos}CD90^{pos}CD105^{pos}$ MSCs (Supplemental Figure 9B). In-order to verify that $CD45^{neg}CD73^{pos}CD90^{pos}CD105^{pos}$ cells are MSCs these cells were isolated from the liver and lung and cultured. These cells displayed typical behavior of MSCs, differentiating into chondrocytes, adipocytes, bone and smooth muscle (Supplemental Figure 9A).

Discussion

In this study we show that Abi3bp is necessary for the co-ordination of proliferation and differentiation of MSCs. (Supplementary Figure 6).

It is clear from our data that Abi3bp is an important determinant of MSC cell biology. Abi3bp was found to promote the rapid turnover of focal adhesions and reduce cellular stress arising from the extracellular matrix. Such changes in cell biology are critically important for differentiation. For example, hepatocyte de-differentiation occurs via cellular flattening, a process involving the integrin receptor α5β1 and fibronectin [22]. More relevantly, using a microimprinting technique to force MSCs to maintain a rectangular or pentagonal shape affected whether the cells developed down an osteogenic or adipogenic pathway [23]. Similarly, MSC elongation was found to be necessary for myogenic differentiation [24]. The amount of cellular tension, as mediated by RhoA, also affects whether an MSC develops into an adipocyte or osteoblast [25].

Proliferation and differentiation are often regarded as two sides of the same coin. Differentiation occurs once the cell stops proliferating. Our results support this hypothesis and show that MSCs require Abi3bp to switch from a proliferative to differentiating state. In the absence of Abi3bp, the integrin-β1 is maintained in a non-active state and the lack of phosphorylated paxillin prevents sequestration of Src and ERK at the plasma membrane, leaving these kinases to activate cyclin-d1 and drive proliferation. Once Abi3bp is present in sufficient amount integrin-β1 is activated and drives paxillin phosphorylation. The phosphorylated paxillin binds to Src and ERK, and by localizing these kinases at the plasma membrane prevents cyclin-d1 activation in the nucleus. Proliferation stops and the MSC enters into a differentiation pathway, as evidenced by the failure of Abi3bp knockout MSCs to differentiate. This has been observed in other cell types, for example integrin-β1 activation and paxillin phosphorylation have been shown to be important for Schwann cell differentiation [26]. Proliferation of MSCs was not important for their transformation ability, Akt-MSCs lacking Abi3bp, which had a higher proliferative state than control cells, had a highly significant reduced rate of transformation (Supplementary Figure 7B). This is important information considering the use of MSCs as therapeutic agents.

With respect to the mechanism it is worth bearing in mind that several experiments rely on the MSC-GFP-Akt1 cell system. In MSC-GFP-Akt1 cells Abi3bp binds to integrin-β1, elevates p-paxillin, which in turn inhibits p-ERK and proliferation through sequestration of Src. These findings are applicable to unmodified MSCs. We found that Abi3bp knockout MSCs were more proliferative than their wild-type counterparts. Similarly, p-ERK and cyclin-d1 were increased by Abi3bp knockout and likewise p-paxillin levels were reduced. Furthermore by chemical inhibition we showed that MSC proliferation is dependent upon Src and ERK.

In the Abi3bp knockout mouse we found elevated MSCs numbers and proliferation in the bone marrow, lung, and liver. However we did not observe any obvious phenotype. The properties of MSCs in vivo remains elusive [27]. MSCs in the bone marrow exert important effects upon hematopoiesis. In our knockout animal we do observe a small increase in eosinophil number within the bone marrow suggestive of the possibility that increased MSC numbers may alter the balance of hematopoiesis. Few studies exist regarding the role of MSCs in the lung and liver (reviewed in [28]. Mouse strains have remarkably dissimilar numbers of MSCs, for example the bone marrow of FVB mice have 10-fold higher MSC numbers than that of C57BL/6 [29]. Yet, there is no correlation with longevity, nor obvious differences in pathology in any organ between these strains suggesting that elevated MSC number may not lead to an obvious phenotype. Considering the lack of phenotype in these tissues we are currently investigating whether injury models will clarify MSC functions in these organs.

Conclusion

In summary, we have identified Abi3bp as a new extracellular matrix protein necessary for the switch from proliferation to differentiation in MSCs. By binding to the integrin-β1 Abi3bp blocks MSCs from proliferating and co-ordinates entry into a differentiation mechanism.

Supplementary Material

Refer to Web version on PubMed Central for supplementary material.

Acknowledgments

We would like to thank the DHVI and John Wong for the use of their flow cytometers. This work was supported by the NIH.

References

1. Hodgkinson CP, Gomez JA, Mirotsou M, et al. Genetic engineering of mesenchymal stem cells and its application in human disease therapy. Hum Gene Ther. 2010; 21:1513–1526. [PubMed: 20825283]
2. Alfaro MP, Pagni M, Vincent A, et al. The Wnt modulator sFRP2 enhances mesenchymal stem cell engraftment, granulation tissue formation and myocardial repair. Proc Natl Acad Sci U S A. 2008; 105:18366–18371. [PubMed: 19017790]
3. Burchfield JS, Iwasaki M, Koyanagi M, et al. Interleukin-10 from transplanted bone marrow mononuclear cells contributes to cardiac protection after myocardial infarction. Circ Res. 2008; 103:203–211. [PubMed: 18566343]
4. Strauer BE, Brehm M, Zeus T, et al. Repair of infarcted myocardium by autologous intracoronary mononuclear bone marrow cell transplantation in humans. Circulation. 2002; 106:1913–1918. [PubMed: 12370212]
5. Salem HK, Thiemermann C. Mesenchymal stromal cells: current understanding and clinical status. Stem Cells. 2010; 28:585–596. [PubMed: 19967788]
6. Gnecchi M, He H, Liang OD, et al. Paracrine action accounts for marked protection of ischemic heart by Akt-modified mesenchymal stem cells. Nat Med. 2005; 11:367–368. [PubMed: 15812508]
7. Mirotsou M, Zhang Z, Deb A, et al. Secreted frizzled related protein 2 (Sfrp2) is the key Akt-mesenchymal stem cell-released paracrine factor mediating myocardial survival and repair. Proc Natl Acad Sci U S A. 2007; 104:1643–1648. [PubMed: 17251350]
8. Matsuda S, Iriyama C, Yokozaki S, et al. Cloning and sequencing of a novel human gene that encodes a putative target protein of Nesh-SH3. J Hum Genet. 2001; 46:483–486. [PubMed: 11501947]
9. Cheng TW, Gong Q. Secreted TARSH regulates olfactory mitral cell dendritic complexity. Eur J Neurosci. 2009; 29:1083–1095. [PubMed: 19302145]
10. Manabe R, Tsutsui K, Yamada T, et al. Transcriptome-based systematic identification of extracellular matrix proteins. Proc Natl Acad Sci U S A. 2008; 105:12849–12854. [PubMed: 18757743]
11. Cerutti JM, Delcelo R, Amadei MJ, et al. A preoperative diagnostic test that distinguishes benign from malignant thyroid carcinoma based on gene expression. J Clin Invest. 2004; 113:1234–1242. [PubMed: 15085203]
12. Terauchi K, Shimada J, Uekawa N, et al. Cancer-associated loss of TARSH gene expression in human primary lung cancer. J Cancer Res Clin Oncol. 2006; 132:28–34. [PubMed: 16205947]
13. Latini FR, Hemerly JP, Oler G, et al. Re-expression of ABI3-binding protein suppresses thyroid tumor growth by promoting senescence and inhibiting invasion. Endocr Relat Cancer. 2008; 15:787–799. [PubMed: 18559958]
14. Wakoh T, Uekawa N, Terauchi K, et al. Implication of p53-dependent cellular senescence related gene, TARSH in tumor suppression. Biochem Biophys Res Commun. 2009; 380:807–812. [PubMed: 19338757]
15. Hodgkinson CP, Mander A, Sale GJ. Protein kinase-zeta interacts with munc18c: role in GLUT4 trafficking. Diabetologia. 2005; 48:1627–1636. [PubMed: 15986239]
16. Nobes CD, Hall A. Rho, rac, and cdc42 GTPases regulate the assembly of multimolecular focal complexes associated with actin stress fibers, lamellipodia, and filopodia. Cell. 1995; 81:53–62. [PubMed: 7536630]
17. Zaidel-Bar R, Ballestrem C, Kam Z, et al. Early molecular events in the assembly of matrix adhesions at the leading edge of migrating cells. J Cell Sci. 2003; 116:4605–4613. [PubMed: 14576354]

18. Wozniak MA, Modzelewska K, Kwong L, et al. Focal adhesion regulation of cell behavior. Biochim Biophys Acta. 2004; 1692:103–119. [PubMed: 15246682]

19. Ren Y, Meng S, Mei L, et al. Roles of Gab1 and SHP2 in paxillin tyrosine dephosphorylation and Src activation in response to epidermal growth factor. J Biol Chem. 2004; 279:8497–8505. [PubMed: 14665621]

20. Sen A, O'Malley K, Wang Z, et al. Paxillin regulates androgen- and epidermal growth factor-induced MAPK signaling and cell proliferation in prostate cancer cells. J Biol Chem. 2010; 285:28787–28795. [PubMed: 20628053]

21. Fabian JR, Daar IO, Morrison DK. Critical tyrosine residues regulate the enzymatic and biological activity of Raf-1 kinase. Mol Cell Biol. 1993; 13:7170–7179. [PubMed: 7692235]

22. Hodgkinson CP, Wright MC, Paine AJ. Fibronectin-mediated hepatocyte shape change reprograms cytochrome P450 2C11 gene expression via an integrin-signaled induction of ribonuclease activity. Mol Pharmacol. 2000; 58:976–981. [PubMed: 11040044]

23. Kilian KA, Bugarija B, Lahn BT, et al. Geometric cues for directing the differentiation of mesenchymal stem cells. Proc Natl Acad Sci U S A. 2010; 107:4872–4877. [PubMed: 20194780]

24. Yang Y, Relan NK, Przywara DA, et al. Embryonic mesenchymal cells share the potential for smooth muscle differentiation: myogenesis is controlled by the cell's shape. Development. 1999; 126:3027–3033. [PubMed: 10357945]

25. McBeath R, Pirone DM, Nelson CM, et al. Cell shape, cytoskeletal tension, and RhoA regulate stem cell lineage commitment. Dev Cell. 2004; 6:483–495. [PubMed: 15068789]

26. Chen LM, Bailey D, Fernandez-Valle C. Association of beta 1 integrin with focal adhesion kinase and paxillin in differentiating Schwann cells. J Neurosci. 2000; 20:3776–3784. [PubMed: 10804218]

27. Nombela-Arrieta C, Ritz J, Silberstein LE. The elusive nature and function of mesenchymal stem cells. Nat Rev Mol Cell Biol. 2011; 12:126–131. [PubMed: 21253000]

28. McQualter JL, Bertoncello I. Concise review: Deconstructing the lung to reveal its regenerative potential. Stem Cells. 2012; 30:811–816. [PubMed: 22331696]

29. Phinney DG, Kopen G, Isaacson RL, et al. Plastic adherent stromal cells from the bone marrow of commonly used strains of inbred mice: variations in yield, growth, and differentiation. J Cell Biochem. 1999; 72:570–585. [PubMed: 10022616]

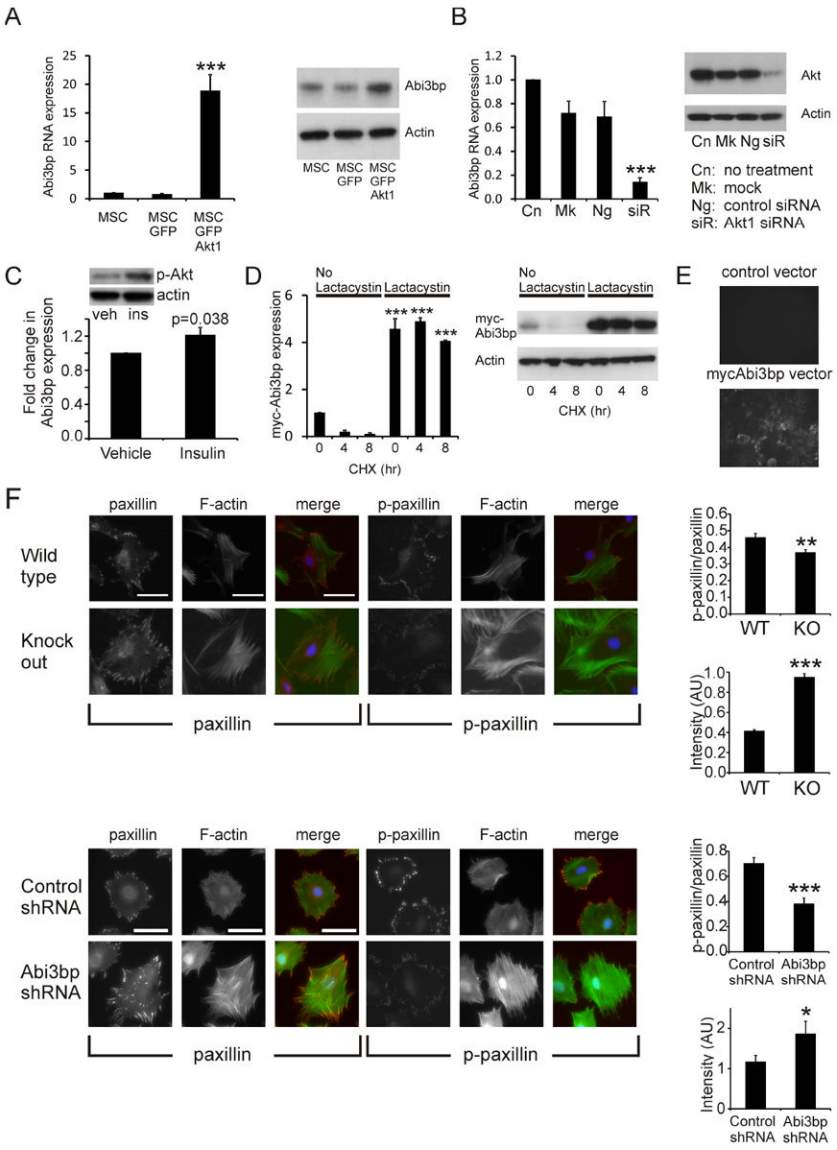

Figure 1. Abi3bp is an extracellular matrix protein which controls MSC cell biology and is regulated by both Akt1 and a post-translational mechanism

(A) MSC, MSC-GFP, MSC-GFP-Akt1 cells, 2 days post-seeding, were analysed for Abi3bp RNA expression by qPCR (left panel n=3) or Abi3bp protein expression (middle panel, n=3). A representative blot is shown far right. Actin was used as a loading control. (B) MSC-GFP-Akt1 cells were transfected with a Akt1 siRNA pool (siR), a negative control siRNA (Ng), the lipid carrier (Mk) or left untreated (Cn) and after 3 days RNA extracted to measure Abi3bp mRNA levels by qPCR. Protein extracts were immunoblotted for Akt1. A representative immunoblot is shown with actin as a loading control. N=3. A and B significance shown for comparisons with control cells, *** $p \leq 0.001$. (C) MSCs were induced with 100nM insulin for 6 hours, following a 4 hour period of serum withdrawal. Extracts were analysed for Abi3bp RNA expression by qPCR. N=3. Inset: phospho-Akt S473 five minutes after insulin stimulation. (D) HEK293 cells over-expressing myc-tagged Abi3bp were treated for 24 hours with vehicle or 1μg/ml clasto-lactacystin β-lactone. Cells were then incubated with either 50μg/ml cycloheximide (CHX) or 50μg/ml cycloheximide with 1μg/ml clasto-lactacystin β-lactone for the indicated times. Cell extracts (20μg) were

probed with a myc antibody or an actin antibody as loading control. N=3. Intensities were normalized to the loading control and normalized intensity of vehicle 0hr was taken to be 1. Significance shown for comparisons with un-treated 0hr cells, *** p≤0.001. (E) HEK293 cells expressing either the control or myc-tagged Abi3bp vector were cultured for 3 days on glass well dishes. Cells were removed by non-enzymatic means and the glass surface probed with a myc antibody. Visualisation was performed with an Alexa Fluor 488 secondary antibody (n=10). (F) MSCs were stained for phospho-paxillin (Y118), paxillin, vinculin, phalloidin or DAPI one day post-seeding. Foci intensity, number, and area as well as phalloidin intensity and cell area were determined. Top panel: representative images for wild-type and Abi3bp knockout MSCs (second isolation). Bottom panel: representative images for MSC-GFP-Akt1 cells. In both cases foci area is expressed as a function of total cell area, with the p-paxillin/paxillin ratio shown and phalloidin intensity in arbitrary units (AU). Scale bar 100microns. N=9-12 for foci area, n=27-36 for phalloidin measurements. Significance between control and Abi3bp knockdown/knockout *p≤0.05, *** p≤0.001.

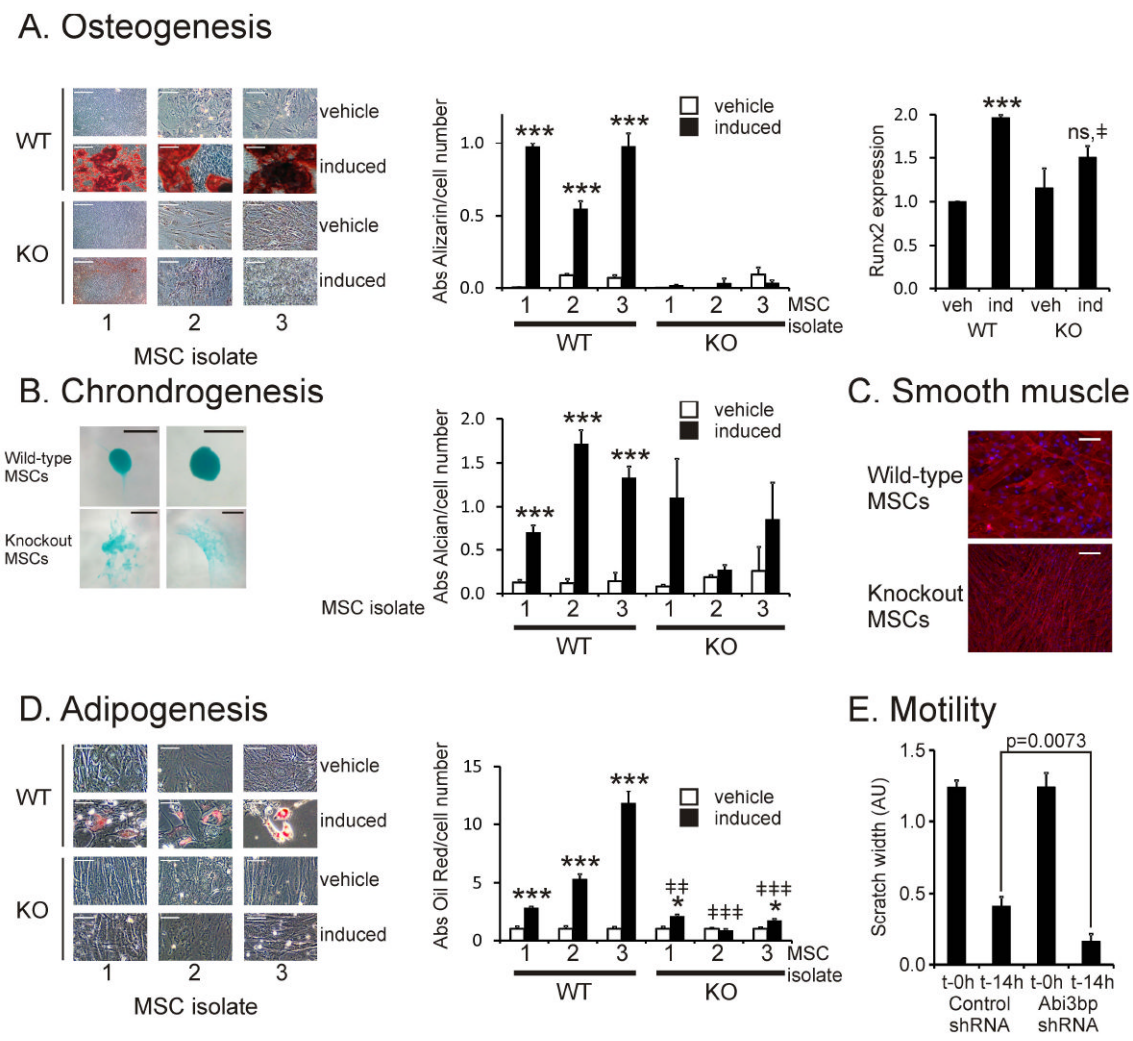

Figure 2. Abi3bp regulates MSC differentiation and motility

(A) Osteogenesis. The three wild-type and Abi3bp knockout MSC isolations were evaluated for alizarin red deposition following osteogenic differentiation, n=5, scale bar 200 microns. Alizarin red staining was normalized to cell number using an MTS assay n=5. *** p≤0.001. Right: RNA, extracted at this time point, was analyzed for Runx2 expression (n=3) *** comparison between vehicle and induced p≤0.001, ‡comparison between WT and KO induced cells p≤0.05. (B) Chondrogenesis. Wild-type and Abi3bp knockout MSC isolates were stained with alcian blue following differentiation, n=3, scale bar 100 microns. Alcian blue staining was normalized to cell number using an MTS assay, n=5. *** p≤0.001 comparison between vehicle and induced (C) Wild-type and Abi3bp knockout MSCs were differentiated to smooth muscle, n=5, scale bar 100 microns. (D) Adipogenesis. MSCs from the wild-type and Abi3bp knockout isolations were stained with Oil Red following differentiation, n=5, scale bar 100 microns. Oil Red staining was normalized to cell number using crystal violet, n=5. *p≤0.001 comparison between vehicle and induced, *** p≤0.001, * p≤0.05. ‡comparison between WT and KO induced cells, ‡‡‡p≤0.001, ‡‡p≤0.01. (E) MSC-GFP-Akt1 cells expressing either scrambled or Abi3bp shRNA were used in a scratch assay. The width of the scratch was measured at t=0h and t=14h (N=9).

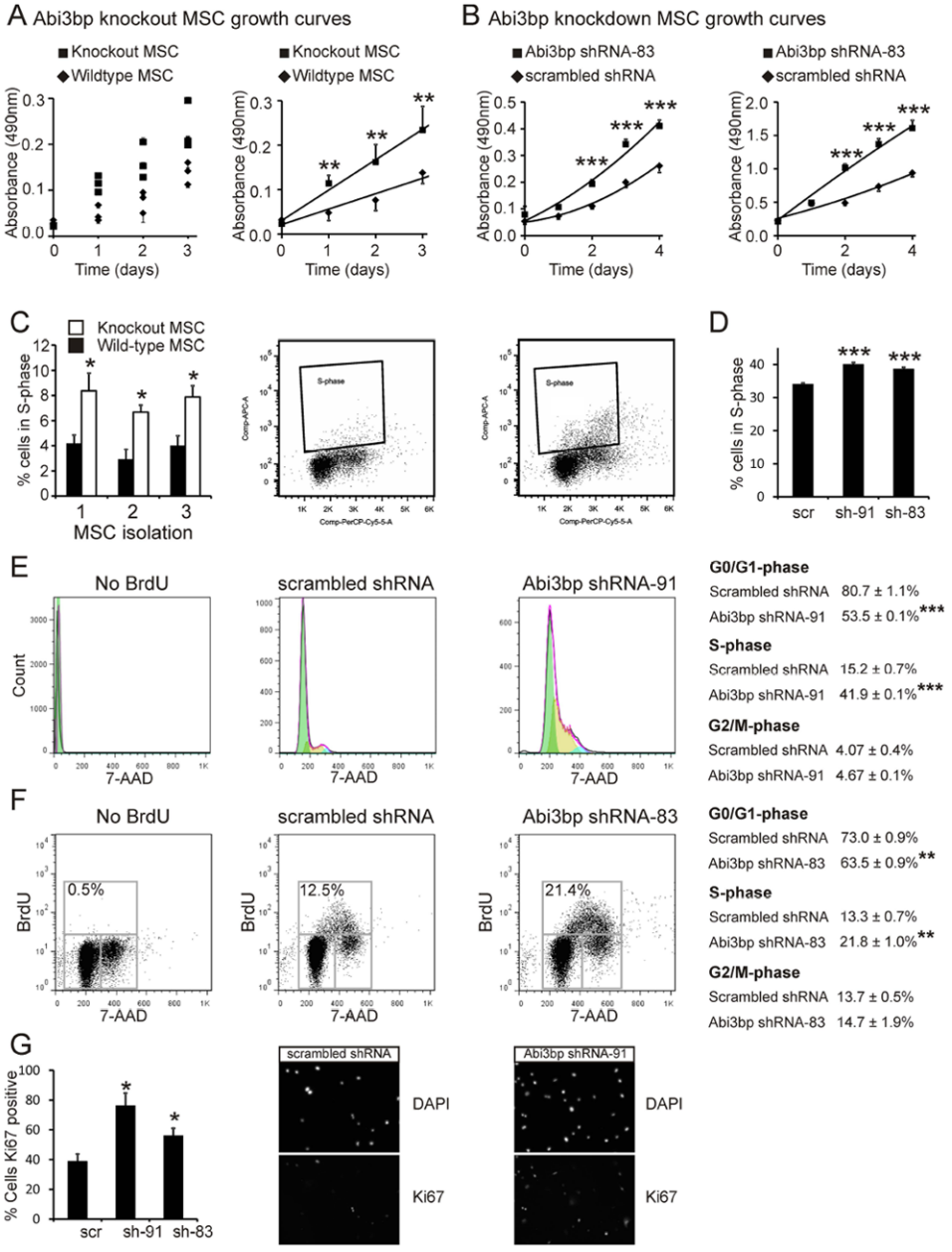

Figure 3. Abi3bp knockout increases MSC proliferation

(A) Left: MTS growth assay curves for the three wild-type and Abi3bp knockout MSC isolations. N=4. Right: Averaged growth rate of the three wild-type and Abi3bp knockout MSCs. (B) MTS assay growth curves for MSCs (left) or MSC-GFP-Akt1 cells (right) expressing scrambled or a Abi3bp shRNA. N=6-7. Comparisons between groups at the same time point, *** p≤0.001. (C) Wild-type and Abi3bp knockout MSCs were incubated with BrdU for 2 hours and analyzed by flow cytometry. BrdU positive cells were in S-phase. N=3. (D) MSC cells expressing scrambled or Abi3bp shRNA were incubated with BrdU and analysed by flow cytometry. MSC-GFP-Akt1 cells expressing scrambled or Abi3bp shRNA-91 were incubated with BrdU. Cells were analyzed for DNA content (E) or BrdU incorporation (F). In (E) cell cycle phases were calculated using a Watson model. In (F) cell

cycle phases are shown on the figure. (E) and (F) N=3, *** p≤0.001. (G) MSC-GFP-Akt1 cells assayed for Ki67. N=3. Comparisons to control cells, *p≤0.05.

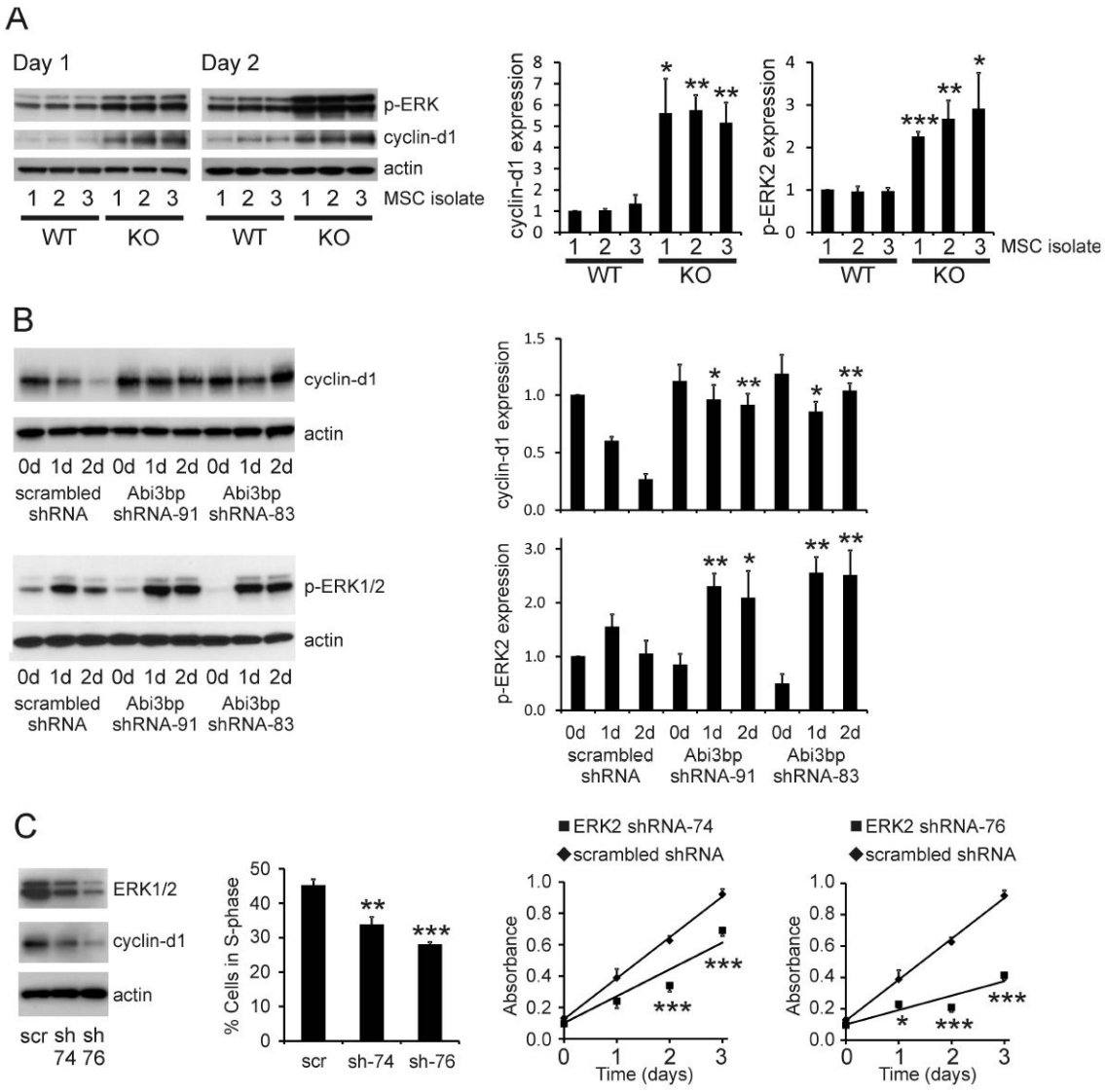

Figure 4. Abi3bp regulates cyclin-d1 expression and ERK phosphorylation

(A) Extracts (7.5μg) from wild-type and Abi3bp knockout MSC isolates, one and two days post seeding, were immunoblotted for p-ERK1/2 and cyclin-d1. Actin was used as a loading control. Intensities were normalized to actin; normalized intensity of wild-type isolation 1 was taken to be 1. (B) Extracts (7.5μg) of MSC-GFP-Akt1 cells expressing either control scrambled or Abi3bp shRNA at zero, one, and two-days post-seeding were probed for cyclin-d1 or phospho-ERK1/2. Actin was used as a loading control. Intensities were normalized to the loading control; normalized intensity of scrambled control cells at day 0 was taken to be 1. N=3 (cyclin-d1), N=4 (p-ERK). Comparisons between groups at the same time point *p≤0.05, ** p≤0.01. (C) Stable knockdown of ERK2 by shRNA. Far left panel: immunoblotting ERK n=4. Left panel: Cells were incubated with BrdU for 6 hours one day post seeding. Percentage of cells in S-phase determined by flow cytometry. N=4. Comparisons between knockdown and control cells ** p≤0.01, *** p≤0.001. Right panels: MTS assay growth curves. N=5. Comparisons between groups at the same time point *p≤0.05, *** p≤0.001.

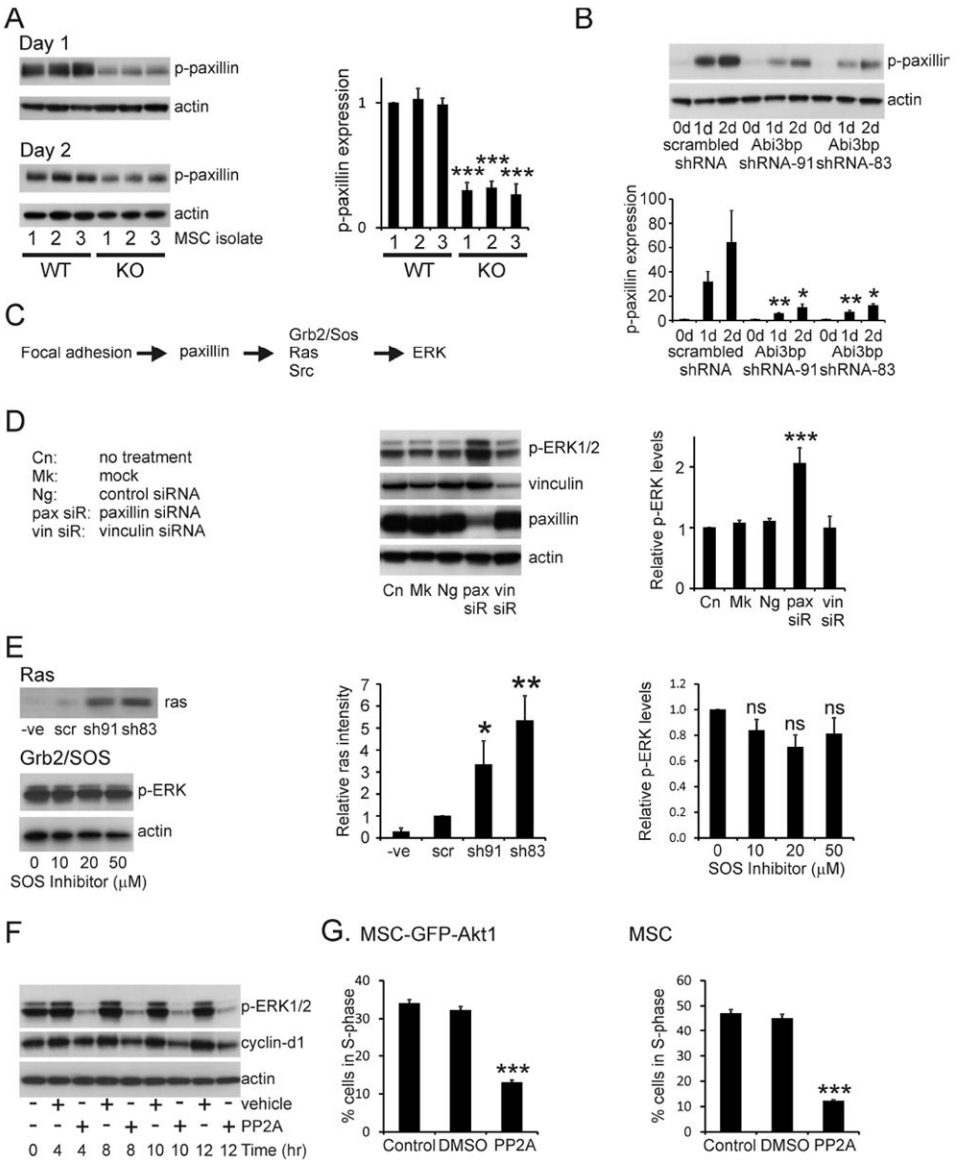

Figure 5. Abi3bp regulates proliferation via Paxillin and Src

(A) Extracts (7.5μg) from the wild-type and Abi3bp knockout MSC isolates, one and two days post seeding, were immunoblotted for pY118-paxillin. Actin was used as a loading control. Intensities were normalized to actin; normalized intensity of wild-type isolation 1 was taken to be 1. (B) Extracts MSC-GFP-Akt1 extracts (7.5μg) cells were probed for phospho-paxillin (Y118) and actin. Phospho-paxillin intensities were normalized to the actin loading control and the normalized intensity of scrambled control cells at day 0 was taken to be 1. N=3. Comparisons between groups at the same time point *p≤0.05, ** p≤0.01. (C) Schematic outline of how focal adhesions and paxillin can influence ERK activity. (D) MSC-GFP-Akt1 cells were transfected with a paxillin siRNA pool (siR), a vinculin siRNA pool, a negative control siRNA (Ng), the lipid carrier (Mk) or left untreated (Cn). After 3 days protein extracts (7.5μg) were probed for phospho-ERK1/2, paxillin, or actin. Intensities were normalized to the actin loading control and the normalized intensity of control cells was taken to be 1. N=3. Significance shown for comparisons between treated groups and control cells ** p≤0.01, *** p≤0.001. (E) Top and middle: Extracts prepared from MSC-

GFP-Akt1 cell two-days post-seeding were incubated with Raf-1-RBD beads. Complexes were extensively washed and probed for ras. A negative control was performed by incubating the Abi3bp-sh83 extract with 1mM GDP. Scrambled control intensity was taken to be 1. N=4. Comparisons to the negative control *p≤0.05, ** p≤0.01. Bottom and far right: MSC-GFP-Akt1 cells, one day post-seeding, were incubated with the indicated concentrations of the Grb2-SOS peptide inhibitor for 12 hours. Extracts (7.5μg) were probed for phospho-ERK1/2 and actin. phospho-ERK intensities were normalized to the actin loading control and the normalized intensity of the untreated cells was taken to be 1. N=5. Comparisons between treated groups and control cells. (F) MSC-GFP-Akt1 cells, one day post-seeding, were incubated with either 10μM PP2, or an equivalent volume of vehicle for the indicated times. Extracts (7.5μg) were probed for phospho-ERK1/2, cyclin-d1, and actin. N=4. Representative image shown. (G) MSC-GFP-Akt1 cells or MSCs, one day post-seeding, were incubated with either 10μM PP2, or an equivalent volume of vehicle for 10 or 12 hours respectively. BrdU was added 4 hours or 8 hours respectively prior to the end of the experiment. Flow cytometry was performed to determine the number of cells in S-phase, n=4. Comparisons to control cells *** p≤0.001.

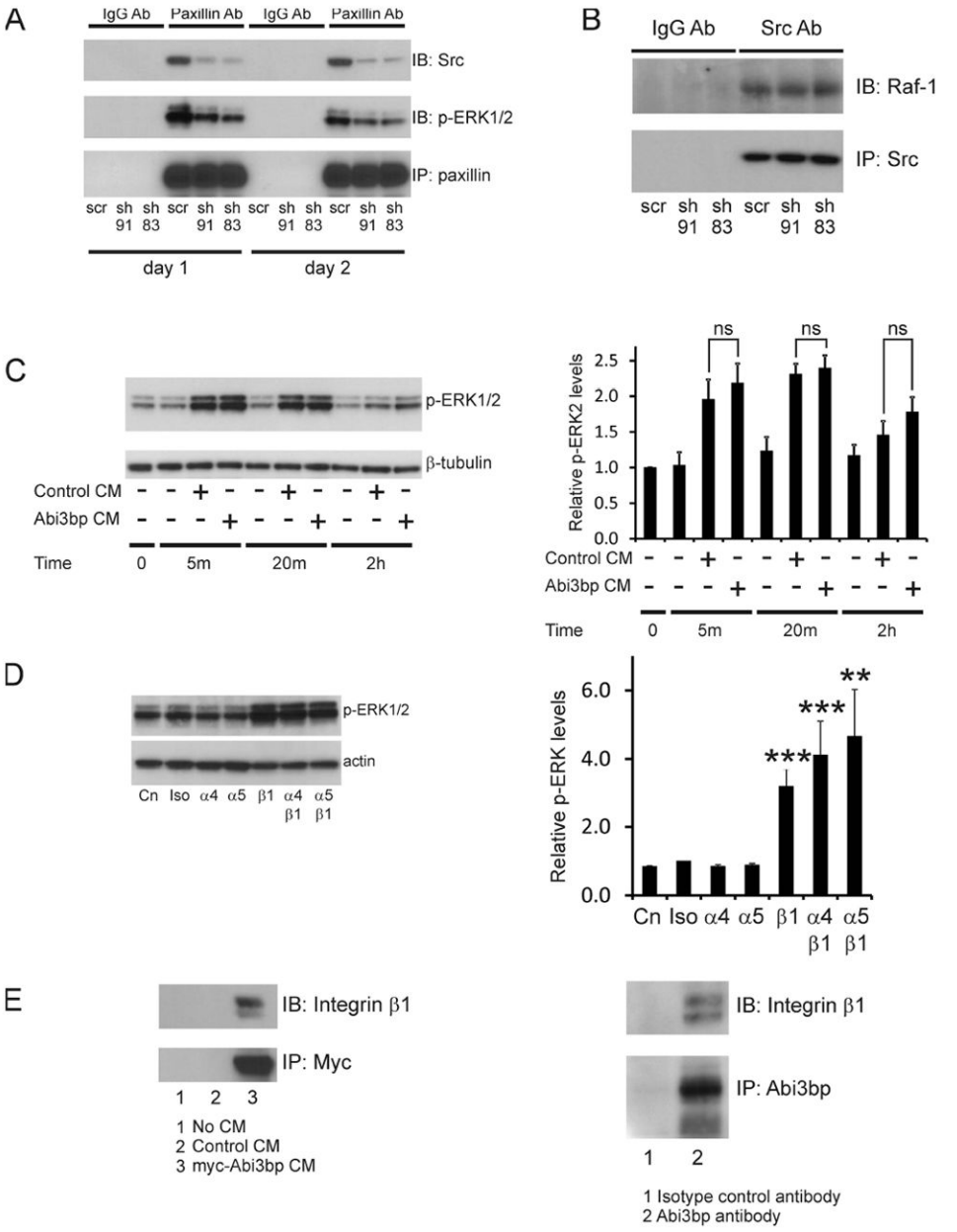

Figure 6. Abi3bp binds to integrin-β1

(A) Extracts prepared from MSC-GFP-Akt1 cells expressing scrambled or Abi3bp shRNA, one and two-days post-seeding, were incubated with either a paxillin or an isotype control antibody. After incubation with protein G beads complexes were extensively washed and probed for Src or phospho-ERK1/2. N=3. Representative image shown. (B) Extracts prepared from MSC-GFP-Akt1 cells expressing scrambled or Abi3bp shRNA at two-days post-seeding after paxillin removal by immunoprecipitation were incubated with either a Src or an isotype control antibody. After incubation with protein G beads complexes were extensively washed and probed for Raf-1. N=3. Representative image shown. (C) Serum starved MSC-GFP-Akt1 cells were treated with either control or Abi3bp conditioned media for the indicated times. Extracts (7.5μg) were probed phospho-ERK1/2 or β-tubulin. N=3. Comparisons are shown, ns- not significant. (D) MSC-GFP-Akt1 cells, one day post-seeding, were incubated with the isotype control antibody (iso) or the indicated integrin

antibodies for 10 hours at 10μg/ml. Extracts (7.5μg) were probed for phospho-ERK1/2 or actin. Total phospho-ERK intensities were normalized to the actin loading control and the normalized intensity of control cells (no addition) was taken to be 1. Comparisons between antibody treated samples and control cells (Cn) **p≤0.01, ***p≤0.001. (E) Left: Extracts prepared from MSC-GFP-Akt1 cells two-days post-seeding were incubated with conditioned media prepared from fresh serum-free media, serum-free media exposed to HEK293 cells expressing the empty vector, or serum-free media exposed to HEK293 cells expressing the myc-tagged Abi3bp vector. After incubation with myc-antibody beads complexes were extensively washed and probed for integrin-β1. N=3. Right: Extracts prepared from MSC-GFP-Akt1 cells, one day post-seeding, were incubated with either a Abi3bp or an isotype control antibody. After incubation with protein G beads complexes were extensively washed and probed for integrin-β1. N=3. Representative image shown.

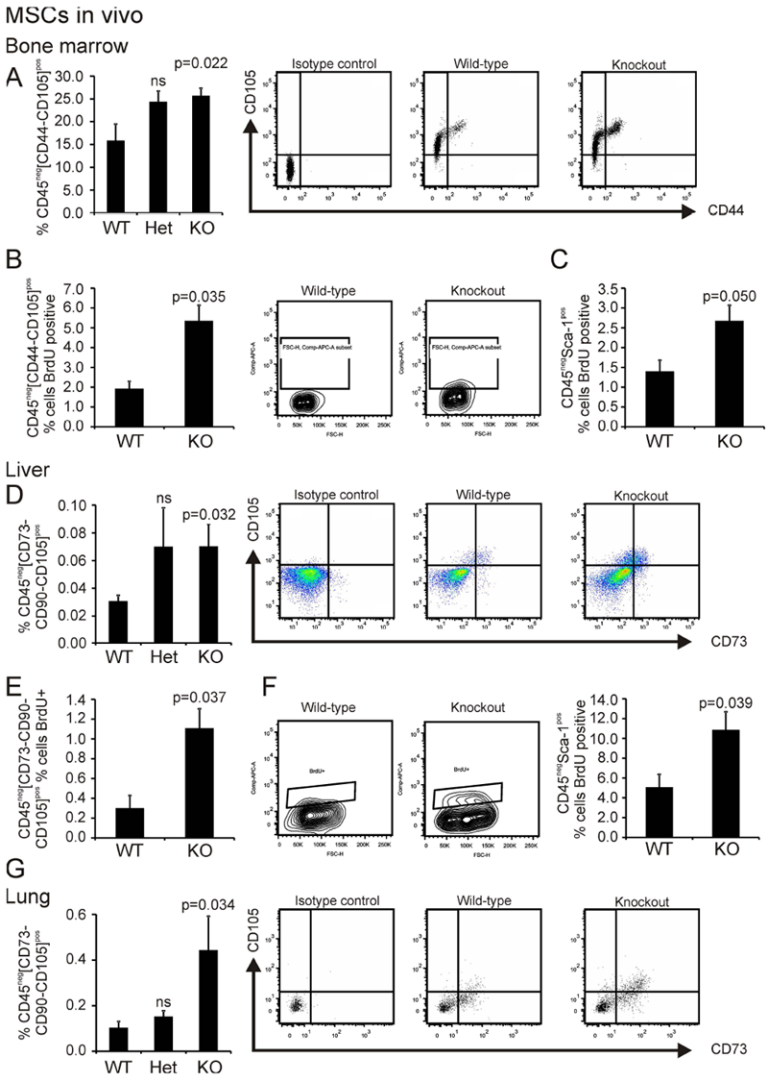

Figure 7. Abi3bp controls MSC proliferation in the bone marrow, lung and liver

(A) Bone marrow aspirates (n=5) were profiled by flow cytometry. MSCs, defined as $CD45^{neg}CD44^{pos}CD105^{pos}$, are presented as a percentage of the total $CD45^{neg}$ population. Wild-type and Abi3bp knockout mice were injected with BrdU and 24 hours later aspirates from the bone marrow collected. BrdU positive MSCs were determined by flow cytometry. (B) Percent $CD45^{neg}CD44^{pos}CD105^{pos}$ MSCs BrdU positive. (C) Percent $CD45^{neg}Sca\text{-}1^{pos}$ MSCs BrdU positive. N=3 and 6. (D) Liver homogenates (N=7) were profiled by flow cytometry. MSCs, defined as $CD45^{neg}CD73^{pos}CD90^{pos}CD105^{pos}$ are presented as a percentage of the total $CD45^{neg}$ population. Livers from BrdU labelled mice were analyzed for MSC BrdU incorporation. (E) Percent $CD45^{neg}CD73^{pos}CD90^{pos}CD105^{pos}$ MSCs BrdU positive. (F) Percent $CD45^{neg}Sca\text{-}1^{pos}$ MSCs BrdU positive. N=3 and 6. (G) Lung homogenates (N=6) were profiled by flow cytometry. MSCs, defined as $CD45^{neg}CD73^{pos}CD90^{pos}CD105^{pos}$ are presented as a percentage of the total $CD45^{neg}$ population.